MINIMAL EDGE PIECEWISE LINEAR KNOTS

J. A. CALVO

Department of Mathematics, University of California,
Santa Barbara, CA 93106, USA

K. C. MILLETT

Department of Mathematics, University of California,
Santa Barbara, CA 93106, USA

The space of n-sided polygons embedded in three-space consists of a smooth manifold in which points correspond to piecewise linear or "geometric" knots, while paths correspond to isotopies which preserve the geometric structure of these knots. Two cases are considered: (i) the space of polygons with varying edge length, and (ii) the space of equilateral polygons with unit-length edges. In each case, the spaces are explored via a Monte Carlo search to estimate the distinct knot types represented. Preliminary results of these searches are presented. Additionally, this data is analyzed to determine the smallest number of edges necessary to realize each knot type with nine or fewer crossings as a polygon, *i.e.* its "minimal stick number."

1. Introduction, vocabulary, and history of geometric knots.

The topological and geometric knotting of circles occurs in many contexts in the natural sciences.[17,25] By geometric knotting we mean the imposition of geometric constraints on allowed configurations and their transformations. These constraints can arise by taking into consideration local "stiffness" of molecular structures such as DNA or other polymers. An attractive structure providing a useful model is that of the spatial polygon. These polygonal configurations are determined by a list of n points in three-space, which we call the *vertices* of the polygon. Straight line segments, or *edges*, connect each successive pairs of vertices, including the first and last one, producing a closed loop. When this configuration is embedded, so that there are no intersections of edges except at common vertices, one has a polygonal knot. The entire collection of such knots determines an open subset of euclidean space whose dimension is three times the number of vertices. Requiring that all vertices lie within the unit cube, that each edge have unit length, or that the angle between adjacent edges be constrained will determine other knot spaces and knot theories of interest.
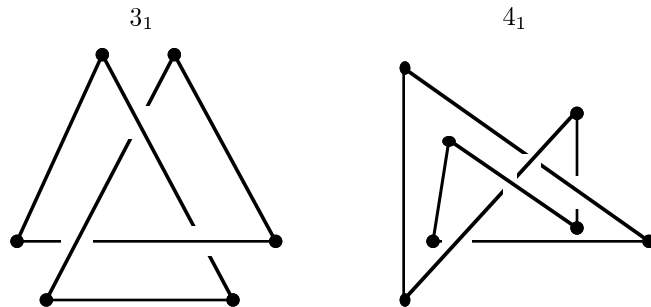
3_1 4_1

Figure 1: A hexagonal trefoil knot and a heptagonal figure eight knot.

1.1. *Minimal stick number*

An n-sided *spatial polygon* P in $\mathbb{R}^3$ is a closed, piecewise linear loop with no self-intersections consisting of n points of $\mathbb{R}^3$, called *vertices,* joined by n straight line segments, called *edges.* We think of an n-gon as the result of glueing n sticks end to end. Define the *minimal stick number $s(K)$* of a topological knot type K as the smallest number of edges required to realize K as a knotted polygon.[1,23] It takes at least six sticks to construct a knotted polygon. A trefoil can be built with six sticks, while at least seven are required to build a figure-eight knot.[a] Thus $s(3_1) = 6$ and $s(4_1) = 7$. Figure 1 shows projections of a hexagonal right-handed trefoil and a heptagonal figure-eight knot. In addition, every five and six crossing prime knot $(5_1, 5_2, 6_1, 6_2, 6_3)$, the square and granny knots $(3_1 \pm 3_1)$, the (3, 4)-torus knot (8_{19}), and the knot 8_{20} can all be built using eight sticks. Figure 2 shows octagonal realizations of these knots. Since only the trefoil and the figure eight can be constructed with fewer edges, all of these knots have stick number $s(\cdot) = 8$. However, it remains an open question whether this is a complete list of the eight-stick knots. Towards this goal, Calvo[5] rules out every possibility other than 8_{18}, which has a minimal stick number of either 8 or 9. In addition to those knots in Figures 1 and 2, all of the seven crossing prime knots $(7_1, \ldots, 7_7)$, as well as knots 8_{16}, 8_{17}, 8_{21}, 9_{40}, and 9_{41} are known to have nine-stick realizations, showing that these knots have minimal stick number $s(\cdot) = 9$.[b]

Formulae for stick number are known only for a couple of families of knots.

---

[a] For instance, see Proposition 1.3 in Millett.[18] In pp.266–268, this proposition is followed not only by pictures, but also by coordinates of the vertices of equilateral realizations of these knots.

[b] The construction of these nine-stick realizations are due to Monica Meissen[15,16] and Robert Scharein[24].

5_1 5_2 6_1

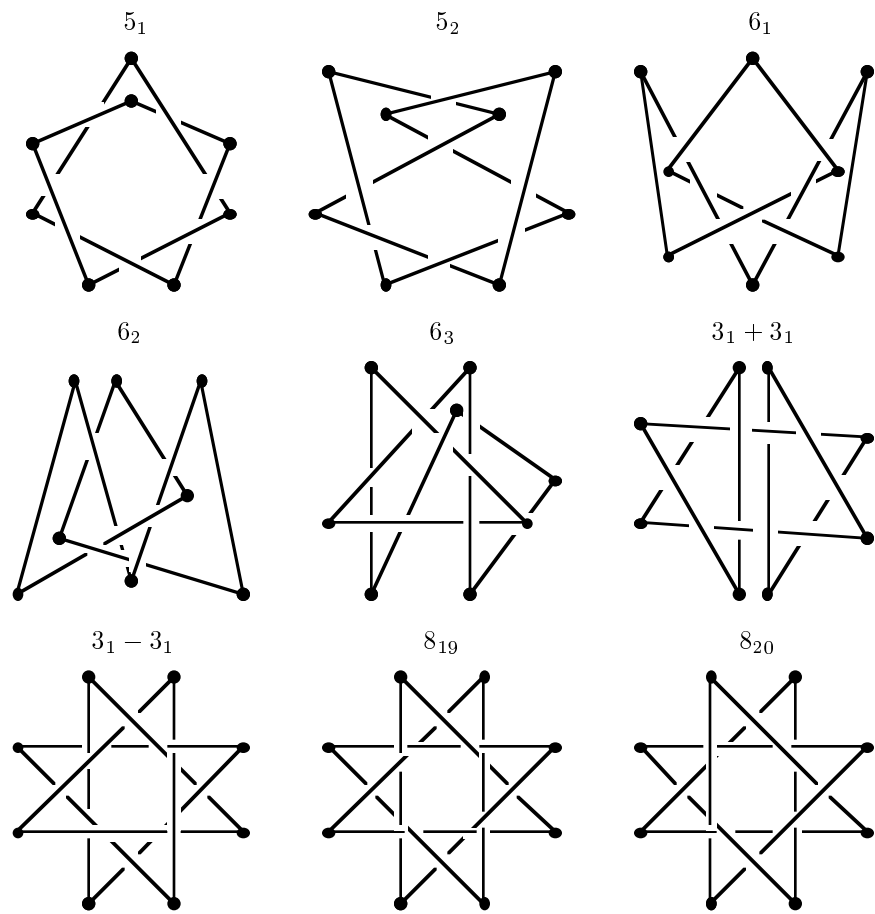6_2 6_3 $3_1 + 3_1$

$3_1 - 3_1$ 8_{19} 8_{20}

Figure 2: Octagonal knots.

Firstly, if p and q are coprime integers with $2 \le p < q < 2p$, the stick number of the (p, q)-torus knot $T_{p,q}$ is

$$s(T_{p,q}) = 2q \qquad (1)$$

(Theorem 7 in Jin[11]). Note that this shows that $s(3_1) = s(T_{2,3}) = 6$ and that $s(8_{19}) = s(T_{3,4}) = 8$. Secondly, the connected sum of any combination of n right- and left-handed trefoils has stick number

$$s(3_1 \pm 3_1 \pm \cdots \pm 3_1) = 2n + 4 \qquad (2)$$

(Theorem 7.1 in Adams *et al*[2]). Thus the square and granny knots have $s(3_1 + 3_1) = s(3_1 - 3_1) = 8$. This is an improvement on the general case of a connected sum, in which

$$s(K_1 + K_2) \le s(K_1) + s(K_2) - 3 \qquad (3)$$

(Theorem 3.1 in Adams *et al*[2]).

Relatively little more is known about stick number. Negami[19] shows that given a nontrivial knot K with crossing number $c(K)$,

$$\frac{5 + \sqrt{9 + 8\,c(K)}}{2} \le s(K) \le 2\,c(K). \qquad (4)$$

Here, the upper bound is obtained using results in graph theory, while the lower bound is found by projecting an n-sided polygon onto a plane perpendicular to one of the edges. The result is an $(n - 1)$-sided polygonal knot diagram having at most $c = \frac{1}{2}n(n-3)$ crossings. Completing the square and solving for n then gives the inequality in (4). Note that the trefoil knot is the only known example for which the upper bound is tight. In fact, Furstenberg *et al*[9] show that if K is a knot with a one-, two-, or three-integer Conway notation and $c(K) > 5$, then this bound can be improved to

$$\frac{5 + \sqrt{9 + 8\,c(K)}}{2} \le s(K) \le c(K) + 2. \qquad (5)$$

On the other side of the spectrum, Jin[11] uses Kuiper's superbridge index $sb(K)$ to obtain the lower bound

$$2\,sb(K) \le s(K). \qquad (6)$$

The superbridge index $sb(K)$ is the minimum over all embeddings of K of the largest number of local maxima obtained when projecting the knot in any direction in $\mathbb{R}^3$ (see Kuiper[12]). Furstenberg *et al*[9] point out that no bound on stick number $s(K)$ gotten from the superbridge index $sb(K)$ can ever be very

efficient. A case in point is the family of two-bridge knots which, by (4), have arbitrarily large stick number but whose superbridge index is bounded above by seven: $sb(K) \leq 7$. Nonetheless, (6) can lead to some interesting bounds. For instance, if $2 \leq p < q$ then the (p,q)-torus knot has $sb(T_{p,q}) = \min\{2p, q\}$ (Theorem B in Kuiper[12]). A systematic construction of polygonal realizations of torus knots then shows that, if $2 \leq p < q$, then

$$2 \min\{2p, q\} \leq s(T_{p,q}) \leq p \left\lceil \frac{2q}{p} \right\rceil, \tag{7}$$

where the "ceiling brackets" denote rounding up, so $\lceil x \rceil = \min\{n \in \mathbb{Z} : n \geq x\}$ (Corollary 5 and Theorem 8 in Jin and Kim[10]). Notice that in the special case when $p = 2r + 1$ and $q = 3r + 1$, we have $2 \min\{2(2r+1), 3r+1\} = 6r + 2$ while $(2r+1)\left\lceil \frac{2(3r+1)}{2r+1} \right\rceil = 6r + 3$. Therefore,

$$6r + 2 \leq s(T_{2r+1, 3r+1}) \leq 6r + 3 \tag{8}$$

for any positive integer r (Corollary 9 in Jin and Kim[10]).

Although here $s(\cdot)$ is defined in the general setting of polygons with arbitrary edge lengths, similar notions of minimal stick number exist for more special sorts of "geometric knots." For instance, one might restrict attention to polygons with unit-length edges, with vertices on the integral lattice $\mathbb{Z}^3$, with restricted vertex angles, or with vertices on the unit-radius sphere about the origin.[c] In this way, stick number might well depend upon the specific type of geometric knot under consideration. For example, Diao[7] has shown that the trefoil knot requires 24 edges for its vertices to lie on the lattice $\mathbb{Z}^3$ and its edges to have unit length. Later, we shall give special attention to equilateral polygons and consider the minimal *equilateral* stick number $s'(K)$ of a topological knot type K. At this time, however, there are no knot types known to have equilateral stick numbers which are different from their standard stick number.

Question 1. How many sticks are required to construct a knot K? In particular, what are the stick numbers for all knots with, say, nine crossings or fewer? Does this depend on whether we use unit-length edges or not?

---

[c] See Adams *et al.*[2]

1.2. *The space of geometric knots*

The general framework for the space of geometric knots was introduced by Randell.[21−22] Consider an n-sided polygon P in $\mathbb{R}^3$, together with a distinguished vertex, or *root*, v_1 and a choice of orientation. We can view P as a point of $\mathbb{R}^{3n}$ by listing the triple of coordinates for each of its n vertices, starting with v_1 and proceeding in sequence as determined by the orientation.

In the spirit of Vassiliev,[3,26] define the *discriminant* $\Sigma^{(n)}$ to be the collection of points in $\mathbb{R}^{3n}$ which correspond in this way to non-embedded polygons. A polygon fails to be embedded in $\mathbb{R}^3$ when two or more of its edges intersect, so $\Sigma^{(n)}$ is the union of the closure of $\frac{1}{2}\,n\,(n-3)$ real semi-algebraic cubic varieties, each consisting of polygons with a given pair of intersecting edges.[d] For example, the collection of polygons $\langle v_1, v_2, \ldots, v_{n-1}, v_n \rangle$ for which $v_1 v_2$ intersects $v_3 v_4$ is the closure of the locus of the system

$$(v_2 - v_1) \times (v_3 - v_1) \cdot (v_4 - v_1) = 0$$
$$(v_2 - v_1) \times (v_3 - v_1) \cdot (v_2 - v_1) \times (v_4 - v_1) < 0$$
$$(v_4 - v_3) \times (v_1 - v_3) \cdot (v_4 - v_3) \times (v_2 - v_3) < 0.$$

In particular, the closure of each of these semi-algebraic varieties forms a codimension-1 submanifold (with boundary) of $\mathbb{R}^{3n}$. Hence the subspace

$$\mathfrak{Geo}^{(n)} = \mathbb{R}^{3n} - \Sigma^{(n)}$$

corresponding to embedded polygons is an open $3n$-manifold which we will call the *embedding space* of rooted oriented n-sided geometric knots.

A path $h : [0, 1] \to \mathfrak{Geo}^{(n)}$ corresponds to an isotopy of polygonal simple closed curves, so each path-component of $\mathfrak{Geo}^{(n)}$ contains polygons of the same topological knot type. If two polygons lie in the same path-component of $\mathfrak{Geo}^{(n)}$, we will say they are *geometrically equivalent*. Also, a polygon is *geometrically unknotted* if it is geometrically equivalent to a standard planar polygon; since all planar n-sided polygons are geometrically equivalent, the component of geometric unknots is well-defined.

The geometric equivalence of two knots implies their topological equivalence. However, not much is known about the converse. For instance, it is unknown whether there exist topological unknots which are geometrically knotted. In fact, until recently there were no known examples of any topological knot type corresponding to two distinct geometric knot types.[e]

---

[d] If $n = 3$, $\Sigma^{(3)}$ is the collection of triangles $\langle v_1, v_2, v_3 \rangle$ for which $(v_2 - v_1) \times (v_3 - v_1) = 0$.

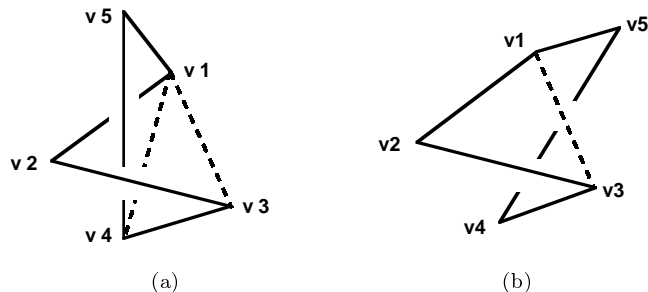[e] See Millett[18] p.265, and compare with Theorem 1 in .[4]

Figure 3: All pentagons are geometric unknots.

Question 2. How many distinct geometric (or topological) knot types are there in $\mathfrak{Geo}^{(n)}$ as a function of n?

Question 3. What can be said about the topology of the components of these knot spaces?

A classical theorem of Whitney[27] guarantees that, for each n, there are only finitely many geometric knot types. Furthermore, it is a "folk theorem" that $\mathfrak{Geo}^{(n)}$ consists of a single path-component when $n \leq 5$. Since triangles are planar, the embedding space $\mathfrak{Geo}^{(3)}$ of rooted oriented triangles is connected. A quadrilateral (tetragon) consists of two triangles hinged along a common edge; since we can change the dihedral angle at the hinge to flatten the quadrilateral out, we find that $\mathfrak{Geo}^{(4)}$ is also connected. Finally, suppose that $P = \langle v_1, v_2, v_3, v_4, v_5 \rangle$ is some pentagon. If the edge $v_4 v_5$ intersects the triangular disc determined by vertices v_1, v_2, and v_3, then P can be deformed by an isotopy of the linkage $v_4 v_5 v_6$ across the disc determined by v_4, v_5, and v_6 until it coincides with the quadrilateral $\langle v_1, v_2, v_3, v_4 \rangle$ (see Figure 3a). On the other hand, if the edge does not intersect that triangle, then P can be deformed by an isotopy of $v_1 v_2 v_3$ across the triangular disc determined by v_1, v_2, and v_3 until it coincides with the quadrilateral $\langle v_1, v_3, v_4, v_5 \rangle$ (see Figure 3b). In either case, P can then be pushed into a plane just like a quadrilateral. Therefore the space $\mathfrak{Geo}^{(5)}$ of pentagons is connected, as well.

The situation when $n = 6$ is described in Calvo.[4–5] In this case, we have to contend with the hexagonal realizations of the trefoil knot. Recall that trefoils are chiral, *i.e.* topologically different than their mirror image. This means that every hexagonal trefoil will lie in a different component of $\mathfrak{Geo}^{(6)}$ than its mirror image. Therefore, there must be at least three distinct path-components in $\mathfrak{Geo}^{(6)}$, corresponding to the unknot, the right-handed trefoil,

7

and the left-handed trefoil. The embedding space $\mathfrak{Geo}^{(6)}$ contains, in fact, five path-components. These consist of a single component of unknots, two components of right-handed trefoil knots, and two components of left-handed trefoil knots. Thus there two distinct geometric realizations of each type of topological trefoil. In particular, hexagonal trefoil knots are not reversible: In contrast with trefoils in the topological setting, reversing the orientation on a hexagonal trefoil yields a different geometric knot. Hence geometric knottedness is actually stronger than topological knottedness.

It turns out that the distinction between the two geometric types of right-handed trefoils is a consequence of our original choice of root and orientation. If we eliminate this choice by taking the quotient of $\mathfrak{Geo}^{(6)}$ modulo the action of the dihedral group of order 12, we find that the spaces of non-rooted oriented hexagonal knots and of non-rooted non-oriented hexagonal knots each consist of three components (Corollary 7 in Calvo [4]). Randell has reported another approach, using a spectral sequence analysis, confirming these results.[f] Nevertheless, the fact that $\mathfrak{Geo}^{(6)}$ consists of five components may prove to be relevant to questions about the topology of DNA, in which there are intrinsic base points and orientations due to the sequences of base pairs.

The classification of hexagonal knots is completed by means of the *joint chirality-curl* $\mathcal{J}$, a combinatorial invariant which distinguishes between all five components of $\mathfrak{Geo}^{(6)}$. In particular, $\mathcal{J}$ takes values as follows:

$$\mathcal{J}(H) = \begin{cases} (0,0) & \text{iff } H \text{ is an unknot,} \\ (+1,\pm1) & \text{iff } H \text{ is a right-handed trefoil,} \\ (-1,\pm1) & \text{iff } H \text{ is a left-handed trefoil.} \end{cases}$$

Reversing orientation on a hexagon will change the sign of the second coordinate of $\mathcal{J}$, while taking mirror its image will change the sign of both coordinates.

The minimal stick number for the figure-eight knot is $s(4_1) = 7$. Thus, the space $\mathfrak{Geo}^{(7)}$ contains at least four path-components containing to the unknot, the right- and left-handed trefoil knots, and the figure eight knot. Topologically, these are the only four knots that can occur with seven edges. Geometrically, there are five heptagonal knot types, two of which correspond to the figure-eight knot (Theorem 4.1 in Calvo [5]). In fact, heptagonal trefoil knots are achiral but not reversible. This is another example demonstrating the difference between topological and geometric knottedness.

Unlike the hexagonal trefoils, though, the irreversibility of heptagonal figure-eights does not depend on our choice of root. In fact, whereas the

---

[f] Personal communication, AMS meeting, Iowa (March 1996).

space of non-rooted non-oriented embedded heptagons consists of four path-components, the space quotient of of non-rooted oriented embedded heptagons consists of five path-components (Corollary 4.7 in Calvo [5]).

Of the nine knot types known to have stick number $s(\cdot) = 8$ (see Figure 2), only two are achiral. Together with the four topological knot types which already occur in $\mathfrak{Geo}^{(7)}$, this gives at least 20 path-components in $\mathfrak{Geo}^{(8)}$. The exact number of geometric – or, for that matter, topological – knot types that can occur when $n = 8$ remains unknown.

1.3. Equilateral polygons

A path in the embedding space $\mathfrak{Geo}^{(n)}$ corresponds to a deformation which can stretch or shrink the edges of a polygon. This type of deformation might be unrealistic when one uses geometric knot theory to model phenomena like DNA molecules. In such cases, we may want a stronger notion of "geometric knot theory" in which the length of the edges remain invariant under deformation. Depending on the relative size of the edges, this new notion of knottedness may actually be different than the more general geometric knottedness described in Section 1.2 above. For instance, Cantarella and Johnston [6] show that for certain choices of edge length, there are "stuck" hexagonal unknots, *i.e.* polygons which are topologically unknotted but cannot be made planar via geometric deformations that preserve edge lengths.

Let us restrict our attention to the class of equilateral polygons and to deformations which preserve the lengths of their edges. Define the embedding space $\mathfrak{Equ}^{(n)}$ of n-sided *equilateral knots* as the collection of polygons $\langle v_1, v_2, \ldots, v_{n-1}, v_n \rangle$ in $\mathfrak{Geo}^{(n)}$ with unit-length edges. Therefore $\mathfrak{Equ}^{(n)}$ is a codimension-n quadric subvariety of $\mathfrak{Geo}^{(n)}$ defined by the equations

$$\|v_1 - v_2\| = \|v_2 - v_3\| = \cdots = \|v_{n-1} - v_n\| = \|v_n - v_1\| = 1.$$

Consider the map $f : \mathfrak{Geo}^{(n)} \to \mathbb{R}^n$ given by the n-tuple

$$f(\langle v_1, v_2, \ldots, v_{n-1}, v_n \rangle) = (\|v_1 - v_2\|, \|v_2 - v_3\|, \ldots, \|v_{n-1} - v_n\|, \|v_n - v_1\|).$$

The point $p = (1, 1, \ldots, 1) \in \mathbb{R}^n$ is a regular value for f (Corollary 1 in Randell [22]), so that $\mathfrak{Equ}^{(n)} = f^{-1}(p)$ is a $2n$-dimensional smooth submanifold which intersects a number of the components of $\mathfrak{Geo}^{(n)}$, some perhaps more than once.

Another helpful way in which to think of the space $\mathfrak{Equ}^{(n)}$ is to use a vector description. An n-sided polygon can be entirely described by its root vertex v_1 and a list of n displacement vectors from one vertex to the next:

$$\vec{V}_1 = v_2 - v_1, \quad \vec{V}_2 = v_3 - v_2, \quad \cdots \quad \vec{V}_{n-1} = v_n - v_{n-1}, \quad \vec{V}_n = v_1 - v_n.$$

Each of these is a unit vector and is, therefore, enumerated by a point of the unit-radius 2-sphere $\mathbb{S}^2$ in $\mathbb{R}^3$. A list of n such vectors is subject to the requirement that their sum is the zero vector in order to ensure a closed polygon. This shows that the collection of n-sided equilateral polygons can be considered to be the codimension-3 subset $\mathcal{S}$ of the product $\mathbb{R}^3 \times \mathbb{S}^2 \times \cdots \times \mathbb{S}^2$ determined by the condition that the sum of the n vectors is zero. Note that $\mathcal{S}$ is a real algebraic variety of dimension $2n$. Then the space $\mathfrak{Equ}^{(n)}$ of equilateral knots is the open subset of $\mathcal{S}$ consisting of the points $(v_1, \vec{V}_1, \vec{V}_2, \cdots, \vec{V}_{n-1}, \vec{V}_n)$ which correspond to embedded polygons.

We will say two polygons are *equilaterally equivalent* if they lie in the same component of $\mathfrak{Equ}^{(n)}$, and that a polygon is an *equilateral unknot* if it is equilaterally equivalent to a standard planar polygon. Millett has shown that all planar polygons are equilaterally equivalent, so the component of equilateral unknots is well-defined.[g]

As in the geometric case, the space $\mathfrak{Equ}^{(3)}$ of triangles is connected; in fact, $\mathfrak{Equ}^{(3)}$ consists of rotations and translations of a rigid equilateral triangle and is thus homeomorphic to $\mathbb{R}^3 \times SO(3)$. All rhombi (equilateral quadrilaterals) are equilaterally unknotted, since we can view a rhombus as the sum of two isosceles triangles "hinged" along one of the rhombus's diagonals. For instance, a rhombus $Q = \langle v_1, v_2, v_3, v_4 \rangle$ corresponds to the sum of the triangles $\langle v_1, v_2, v_3 \rangle$ and $\langle v_3, v_4, v_1 \rangle$. We can move v_2 and keep $\|v_1 - v_2\| = \|v_2 - v_3\| = 1$ by rotating the triangular linkage $v_1 v_2 v_3$ about the axis through v_1 and v_3 until Q lies completely in a plane. Hence $\mathfrak{Equ}^{(4)}$ is connected.

Randell[22] showed that any equilateral pentagon can be deformed to a planar one without changing the length of any of its edges. For suppose $P = \langle v_1, v_2, v_3, v_4, v_5 \rangle$ is an equilateral pentagon. Let $\mathcal{P}$ be the plane determined by vertices v_1, v_2, and v_3. If $\mathcal{P}$ separates v_4 from v_5, then either

  (i) both v_3 and v_4 lie on one side of the plane containing v_1, v_2, and v_5, or
  (ii) both v_1 and v_5 lie on one side of the plane containing v_2, v_3, and v_4.

Thus, after relabeling, we can assume that both v_4 and v_5 lie to one side of $\mathcal{P}$. In this case, rotate the triangular linkage $v_1 v_2 v_3$ about the axis through v_1 and v_3 until it lies coplanar with v_4. We can then deform the quadrilateral linkage $v_1 v_2 v_3 v_4$ in its plane until it misses the line through v_1 and v_4; this is easy to achieve since the set of quadrilateral linkages $v_1 v_2 v_3 v_4$ embedded in the plane forms a connected one-parameter family described entirely by the angle $\angle v_4 v_1 v_2$. We can then rotate the linkage $v_4 v_5 v_1$ about the axis through

---
[g] For example, see steps 2 and 3 in the proof of Proposition 2.1 in Millett.[18]

v_1 and v_4 until the entire pentagon lies in a single plane. Since any equilateral pentagon can be flattened out, $\mathfrak{Equ}^{(5)}$ must also be connected.

Consider the case when $n = 6$. We have equilateral examples of each of the five types of hexagons in $\mathfrak{Geo}^{(6)}$. For example, the regular hexagon

$$H_0 = \langle (1, 0, 0), (.5, .866025, 0), (-.5, .866025, 0),$$
$$(-1, 0, 0), (-.5, -.866025, 0), (.5, -.866025, 0) \rangle$$

is an equilateral unknot, while the hexagon

$$H_1 = \langle (0, 0, 0), (.886375, .276357, .371441),$$
$$(.125043, -.363873, .473812), (.549367, .461959, .845227),$$
$$(.818041, 0, 0), (.4090205, -.343939, .845227) \rangle$$

is an equilateral trefoil with $\mathcal{J}(H_1) = (+1, +1)$. Let ρH and rH denote the mirror image (or obverse) and the reverse of a hexagon H; then ρ, r, and ρr are involutions of $\mathfrak{Geo}^{(6)}$ taking H_1 to equilateral trefoils of the other three types. Therefore $\mathfrak{Equ}^{(6)}$ intersects each of the five components of $\mathfrak{Geo}^{(6)}$ at least once.

The first in-depth analysis of $\mathfrak{Equ}^{(6)}$ was done by Millett and Rosa Orellana. They show that any topologically unknotted equilateral hexagon can be deformed to a planar one without changing the length of any of its edges.[h] Thus $\mathfrak{Equ}^{(6)}$ contains a single component of unknots. Calvo [4−5] completes the study of equilateral hexagons, showing that any two equilateral hexagons are equilaterally equivalent exactly when they are geometrically equivalent. Therefore, $\mathfrak{Equ}^{(6)}$ contains exactly five path-components, consisting of a single component of unknots, two components of right-handed trefoil knots, and two components of left-handed trefoil knots (Theorem 2 in Calvo[4]). As with $\mathfrak{Geo}^{(6)}$, the joint chirality-curl $\mathcal{J}$ distinguishes among these components. Nevertheless, each component of trefoils in $\mathfrak{Equ}^{(6)}$ contains essential loops which are null-homotopic in $\mathfrak{Geo}^{(6)}$, so that the inclusion $i : \mathfrak{Equ}^{(6)} \hookrightarrow \mathfrak{Geo}^{(6)}$ has a nontrivial kernel at the level of fundamental group. Thus, the trefoil components of $\mathfrak{Equ}^{(6)}$ are not homotopy equivalent to those in $\mathfrak{Geo}^{(6)}$ (Theorem 15 in Calvo[4]). In particular, this shows that, despite the fact that equilateral and geometric knot types coincide in the case $n = 6$, the two notions of knottedness are quite different in nature.

Question 4. Are there values of n for which the number of path-components in $\mathfrak{Geo}^{(n)}$ and $\mathfrak{Equ}^n$ differ? This can occur if there exist either topological knot

---

[h] This result is mentioned, for example, in Proposition 1.2 of Millett.[18] An alternate proof is presented in Calvo.[4−5]

types which are realizable only by "scalene" n-sided polygons, or equilateral isotopes of the same geometric knot type.

2. Monte Carlo search methods.

2.1. *Random knot generation*

The complexity of the knot spaces $\mathfrak{Geo}^{(n)}$ and $\mathfrak{Equ}^{(n)}$ has proven to be very difficult to penetrate analytically. Instead, we shall explore these spaces probabilistically, by selecting a large number of "random" configurations in these spaces. As the size of the sample of this Monte Carlo search increases, one obtains a better understanding of the spaces, the topological knot types realized, and the minimal stick numbers of those knots.

Consider generating a random geometric knot in $\mathfrak{Geo}^{(n)}$. By a homothety, any knot type which occurs in $\mathfrak{Geo}^{(n)}$ will be realizable by a polygon in the cube $[0,1]^3$. This allows us to restrict our attention to the subspace $\mathfrak{Geo}^{(n)} \cap [0,1]^{3n}$. In this case, one Monte Carlo approach is quite straight forward. With respect to the uniform distribution on the interval $[0,1]$, one selects a list of $3n$ numbers to represent the coordinates of the n vertices of the polygon. Geometric knots are obtained by connecting these vertices by linear segments cyclically.

A helpful tool in the study of the spaces $\mathfrak{Equ}^{(n)}$ of equilateral knots is the *pivot transformation.* A pivot is determined by a pair of non-adjacent vertices of a polygon, which separate the regular n-gon into two pieces, together with a *pivot angle* $\phi \in [-\pi, \pi]$. The pivot transforms the polygon by holding the image on one of these pieces fixed and rotating the image of the other piece about the axis through the two designated vertices by the given angle. Up to a rotation of euclidean 3-space about the same axis, the result of the pivot will be equivalent to the one given by reversing the roles of the two pieces. Furthermore, if ϕ is sufficiently small, the new polygon will have the same equilateral knot type as the one with which we started. The following two theorems assist in the study of equilateral knot spaces.

Theorem 1. (Proposition 2.1 in Millett[18]) For any two equilateral polygons in $\mathfrak{Equ}^{(n)}$, there is a finite sequence of translations, rotations, and pivots taking one polygon to the other.

This theorem is helpful in the study of Question 2, as it provides a method to construct any possible knot type. If the knots are based at (0,0,0) and the second vertex is (1,0,0), then translations and rotations are not required. Since all knot types have a representative of this sort, pivots are the only transformations required. Similar methods show that any path connecting two

equilateral polygons in $\mathfrak{Equ}^{(n)}$ can be approximated as closely as desired by a sequence of pivots. This implies that the pivots generate all possible paths, a fact of relevance in the study of a geometric knot type.

2.2. *Recognition of knot type*

One important tool in the study of knot spaces has been the calculation of knot invariants that can be used to identify knot types in the standard classification of knots. Historically, the Alexander polynomial has been the principal example, and it continues to be a popular one due to the relative ease of its calculation. Since 1984, however, this has changed with the creation of the Jones polynomial and its successors, the HOMFLY polynomial, the Kauffman polynomial and, more recently, the "quantum" and Vassiliev finite-type invariants. While, in theory, these are impractical due to the complexity of their computation, they actually are remarkably effective in practice. In addition, certain simplifications have proved to be helpful.[20] Based upon the observed computational complexity of, for example, the HOMFLY polynomial, one might make the conjecture: "The invariant of the generic knot is easy to compute."

The HOMFLY polynomial is a finite Laurent polynomial in two variables, l and m, with integer coefficients associated with each topological knot type.[8,13–14] For the 2977 prime knots represented with fewer than 13 crossings there are only 76 cases that have the same first term as the trivial knot. By considering the entire invariant, these are easily eliminated. Furthermore, most – though not all – chiral knots are distinguished by their HOMFLY polynomial.[i] Thus, although there are small families of knots having the same invariant, the HOMFLY polynomial is a good assay for determining topological knot type when dealing with small crossing and stick numbers. For a first estimate, we use distinct HOMFLY polynomials as a surrogate for distinct topological knot type; note that we *do not* identify chiral presentations.

3. **Results of search.**

In this section, we will describe a number of numerical calculations. Many of these are in a rather preliminary and incomplete state. In particular, we address Questions 1 and 2:

- How many distinct knot types are there in $\mathfrak{Geo}^{(n)}$ or $\mathfrak{Equ}^{(n)}$ as a function of the number of vertices?

---

[i] Knot 9_{42} is an example of a chiral knot that has the same HOMFLY polynomial as its mirror image.

- What are the stick numbers $s(K)$ and $s'(K)$ of all knots K with nine or fewer crossings?

For $\mathfrak{Geo}^{(n)}$, partial results of research in progress are shown in Figure 4 and Table 1. In this computation, n points are selected randomly within the unit cube $[0,1]^3$ and connected cyclically by linear segments. The HOMFLY polynomial of the resulting knot is then calculated. The polynomials are counted to estimate the number of distinct knot types.

Figure 4 shows a plot of the number of distinct HOMFLY polynomials observed in $\mathfrak{Geo}^{(n)}$ as a function of n. Note that growth in the number of polynomials gives an estimate of the number of knot types represented. This data clearly indicates the exponential growth in the topological knot types as a function on n. Since, asymptotically, knots are chiral one should divide the number of HOMFLY polynomials by two to estimate the number of topological knot types up to mirror image.

Table 1 displays the observed stick number $s(\cdot)$ for all knots with nine or fewer crossings. Where possible, exact results, such as those discussed in Section 1.1, are given; these are marked by stars ($\star$). Otherwise, the table indicates the smallest n observed in the Monte Carlo search for which a realization of a given knot type exists.

For $\mathfrak{Equ}^{(n)}$, partial results of research in progress are shown in Figure 5 and Table 2. In this case, the pivot transformation is successively applied, beginning at the regular polygon, and the HOMFLY polynomial is calculated. Then the number of distinct polynomials is counted. Figure 5 shows a plot of the number of distinct polynomials obtained in the search of each space, providing a rough estimate for the total number of distinct knot types in $\mathfrak{Equ}^{(n)}$ as a function of n. In addition to exploring $\mathfrak{Equ}^{(n)}$ for the relatively small values of n shown in Figure 5, the Monte Carlo search was also performed for $\mathfrak{Equ}^{(50)}$, in which case realizations of every knot listed in Table 4 were found. However, the exploration of $\mathfrak{Equ}^{(n)}$ for the smaller values of n is still at an early stage. Table 2 displays the observed equilateral stick number $s'(\cdot)$ for all knots with nine or fewer crossings found thus far by these Monte Carlo searches. As in Table 1, minimal stick numbers are marked by stars ($\star$).

For larger n, the computational power that is required to obtain an accurate approximation to the total number of knot types realizable in $\mathfrak{Geo}^{(n)}$ or $\mathfrak{Equ}^{(n)}$ can be overwhelming. In practice, one observes only a fraction of the total number of knot types, even after a large number of observations have been made. For example, the case of fifty edges is shown in Figure 6a, which plots the growth in the number of distinct knot types $\mathcal{K}$ observed as a function of the number t of samples taken. After a total of 13,750,000 Monte Carlo observations in $\mathfrak{Equ}^{(50)}$, a total of 2935 distinct HOMFLY polynomials have

14

Table 1: Observed geometric stick numbers $s(\cdot)$ for knots with nine or fewer crossings. Stars ($\star$) indicate cases for which the minimal stick number is actually known.

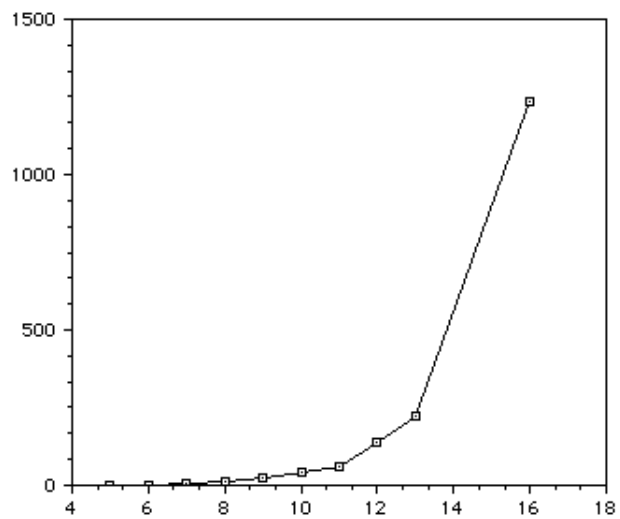| K	s(K)	K	s(K)	K	s(K)
0	$3^\star$	8_{13}	11	9_{22}	14
		8_{14}	11	9_{23}	14
3_1	$6^\star$	8_{15}	12	9_{24}	12
		8_{16}	$9^\star$	9_{25}	15
4_1	$7^\star$	8_{17}	$9^\star$	9_{26}	12
		8_{18}	9	9_{27}	12
5_1	$8^\star$	8_{19}	$8^\star$	9_{28}	12
5_2	$8^\star$	8_{20}	$8^\star$	9_{29}	15
		8_{21}	$9^\star$	9_{30}	13
6_1	$8^\star$	$3_1 + 5_1$	12	9_{31}	13
6_2	$8^\star$	$3_1 - 5_1$	11	9_{32}	12
6_3	$8^\star$	$3_1 + 5_2$	12	9_{33}	12
$3_1 + 3_1$	$8^\star$	$3_1 - 5_2$	12	9_{34}	12
$3_1 - 3_1$	$8^\star$	$4_1 + 4_1$	11	9_{35}	13
				9_{36}	14
7_1	$9^\star$	9_1	13	9_{37}	14
7_2	$9^\star$	9_2	14	9_{38}	15
7_3	$9^\star$	9_3	12	9_{39}	13
7_4	$9^\star$	9_4	14	9_{40}	$9^\star$
7_5	$9^\star$	9_5	13	9_{41}	$9^\star$
7_6	$9^\star$	9_6	13	9_{42}	$9^\star$
7_7	$9^\star$	9_7	12	9_{43}	10
$3_1 + 4_1$	10	9_8	13	9_{44}	10
		9_9	13	9_{45}	10
8_1	10	9_{10}	13	9_{46}	$9^\star$
8_2	11	9_{11}	13	9_{47}	12
8_3	12	9_{12}	12	9_{48}	12
8_4	10	9_{13}	13	9_{49}	11
8_5	12	9_{14}	14	$3_1 + 6_1$	13
8_6	12	9_{15}	11	$3_1 - 6_1$	13
8_7	12	9_{16}	14	$3_1 + 6_2$	14
8_8	11	9_{17}	14	$3_1 - 6_2$	14
8_9	12	9_{18}	13	$3_1 + 6_3$	13
8_{10}	12	9_{19}	13	$4_1 + 5_1$	14
8_{11}	10	9_{20}	13	$4_1 + 5_2$	15
8_{12}	12	9_{21}	14	$3_1 + 3_1 \pm 3_1$	$10^\star$

Figure 4: Growth in the number of distinct HOMFLY polynomials observed in $\mathfrak{Geo}^{(n)}$, plotted as a function of n.
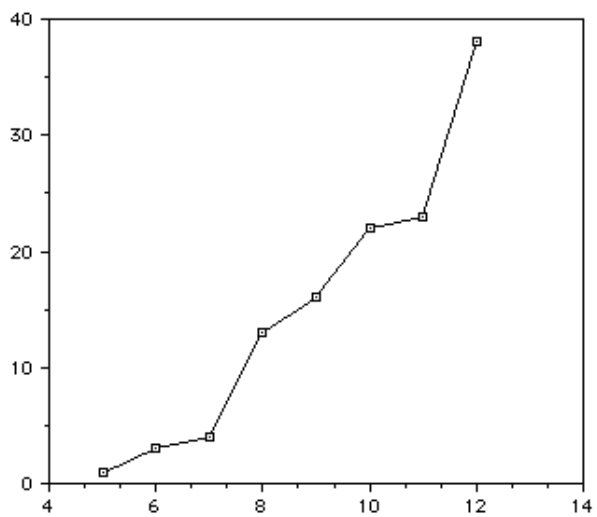

Figure 5: Growth in the number of distinct HOMFLY polynomials observed in $\mathfrak{Equ}^{(n)}$, plotted as a function of n.

16

Table 2: Observed equilateral stick numbers $s'(\cdot)$ for knots with nine or fewer crossings. Stars ($\star$) indicate cases for which the minimal equilateral stick number is actually known.

K	$s'(K)$	K	$s'(K)$
0	$3^\star$	7_3	12
		7_4	12
3_1	$6^\star$	7_5	11
		7_6	12
4_1	$7^\star$	7_7	12
		$3_1 + 4_1$	11
5_1	$8^\star$		
5_2	$8^\star$	8_2	12
		8_{13}	12
6_1	$8^\star$	8_{14}	12
6_2	$8^\star$	8_{19}	9
6_3	$8^\star$	8_{20}	10
$3_1 + 3_1$	9	8_{21}	10
$3_1 - 3_1$	10		
		9_{42}	$9^\star$
7_1	12	9_{45}	14
7_2	12	9_{46}	14

been found. However the shape of the graph indicates that this number is likely to increase significantly after more sampling.

The situation can be likened to a "fish problem," where one wishes to determine the number of species of fish inhabiting a lake via random sampling of the population. The problem, in the case of knots, is complicated by the fact that the relative proportions of species are far from being uniform. One solution is to approximate the observed values of $\mathcal{K}$ with a function which can then be used to estimate the total number of knot types possible. The data collected during the Monte Carlo searches suggests a function of the form

$$\mathcal{K}(t) = N\left(1 - Ae^{-kt}\right). \tag{9}$$

Here the parameter N represents the total number of knot types realizable with n sticks. We consider the sequence of total knot types observed after, say, every 250,000 samples and find the best fitting curve of the form in (9) for these data points. This is done by taking some small integer $j \geq 1$ and considering successive differences of the form

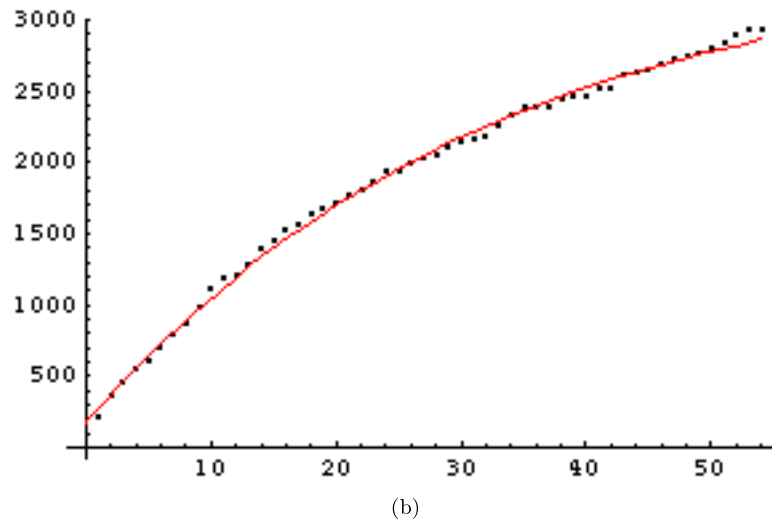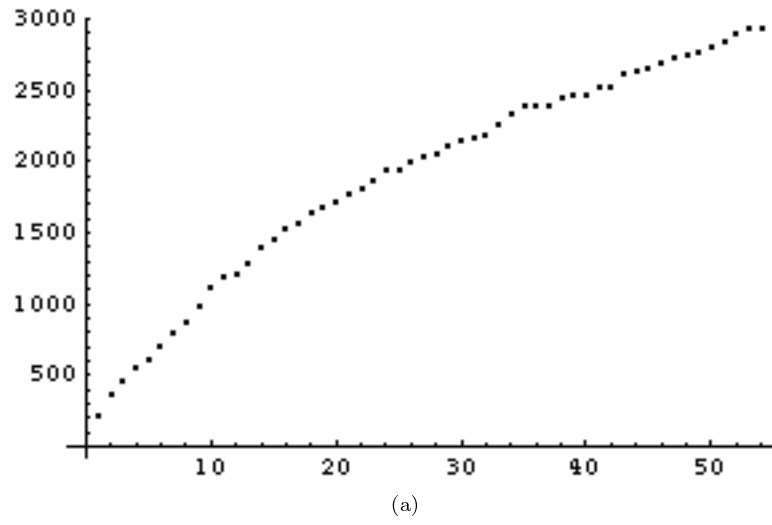$$\mathcal{K}(t + j) - \mathcal{K}(t) = NA\left(1 - e^{-kj}\right)e^{-kt}.$$

(a)

(b)

Figure 6: Growth in the number $\mathcal{K}$ of distinct knot types observed in $\mathfrak{Equ}^{(50)}$ as a function of the number t of samples. Each unit in t corresponds to 250,000 samples.

18

Table 3: Approximate number of knot types N in $\mathfrak{Equ}^{(50)}$.

.

j	N	$\mathbf{R^2}$
1	3471.6	0.997536
2	3701.0	0.997046
3	3828.0	0.996360
4	3826.4	0.996369

A least-squares regression fitting a line to $\ln\left(\mathcal{K}(t+j) - \mathcal{K}(t)\right)$ will then yield a "good" value for the parameter k. The desired parameter N is then found by a second least-squares regression fitting a curve of the form in (9) to the data points of $\mathcal{K}$.

Table 3 shows the approximate total number of knot types N obtained by using $j = 1, 2, 3, 4$ for the Monte Carlo searches for $\mathfrak{Equ}^{(50)}$. The coefficient of determination R^2 for the corresponding curve fit is also indicated in each case.[j] Of these, the better approximation seems to come from $j = 1$, in which case

$$\mathcal{K}(t) = 3471.61 - 3305.46e^{-0.03138t}. \tag{10}$$

Figure 6b shows a plot of this function. This predicts a total of about 3,472 distinct HOMFLY polynomials, providing a conjectured lower bound for chiral knot types in $\mathfrak{Equ}^{(50)}$.

4. Conclusions

The Monte Carlo approach described in Section 2 seems an effective means for producing rough estimates, both in the general case of polygons with arbitrary edge length and in the case of equilateral polygons, of the total number of knot types in each knot space and of the minimal stick number for each topological knot type. In particular, Tables 1 and 2 in Section 3 are the only available compilation of stick number information for all knots with nine or fewer crossings of which we are aware.

---

[j] The coefficient of determination R^2 is a classical statistical tool measuring how well a curve fits a data set. The better the fit, the closer R^2 is to 1. Given a data set $\{p_i\}_{i\in\{1,\ldots,m\}}$ with mean $\bar{p}$ and a curve $q(t)$ approximating it, the coefficient of determination is defined as the ratio

$$R^2 = \frac{\sum_{i=1}^m (p_i - \bar{p})^2 - \sum_{i=1}^m (p_i - q(i))^2}{\sum_{i=1}^m (p_i - \bar{p})^2}.$$

Although the results in Section 3 are only preliminary, one lesson is clear: The amount of sampling required to give an accurate estimates for these quantities will be staggering. For example, consider the data for the Monte Carlo search in $\mathfrak{Cqu}^{(50)}$. After 13,750,000 observations the search has revealed 2935, or about 85%, out of a conjectured 3,472 distinct HOMFLY polynomials. According to the prediction curve (10), it should take an *additional* 20 million observations before finding 98% of the conjectured total.

Of course, deeper statistical analysis of the data, especially in regards to the non-uniform distribution in the population of knot types in these spaces, is likely to yield better information in both these areas.

Acknowledgments

References

1. Adams, C. C., *The Knot Book: An Elementary Introduction to the Mathematical Theory of Knots,* W. H. Freeman and Co., New York (1994).
2. Adams, C. C., B. M. Brennan, D. L. Greilsheimer, and A. K. Woo, *Stick numbers and composition of knots and links,* Journal of Knot Theory and its Ramifications **6** no.2 (1997) 149–161.
3. Birman, J. S. and X. S. Lin, *Knot polynomials and Vassiliev's invariants,* Inventiones Mathematicae **111** (1993) 225–270.
4. Calvo, J. A., *The embedding space of hexagonal knots,* preprint (1998).
5. ———, *Geometric knot theory,* Ph.D. thesis, University of California, Santa Barbara (1998).
6. Cantarella, J. and H. Johnston, *Nontrivial embeddings of polygonal intervals and unknots in 3-space,* preprint (1998).
7. Diao, Y., *Minimal knotted polygons on the cubic lattice,* Journal of Knot Theory and its Ramifications **2** no.4 (1993) 413–425.
8. Freyd, P., D. Yetter, J. Hoste, W. B. R. Lickorish, K. C. Millett, and A. Ocneanu, *A new polynomial invariant of knots and links,* Bulletin of the American Mathematical Society (New Series) **12** no.2 (1985) 239–246.
9. Furstenberg, E., J. Lie, and J. Schneider, *Stick knots,* preprint (1997).

10. Jin, G. T., and H. S. Kim, *Polygonal knots,* Journal of the Korean Mathematical Society **30** no.2 (1993), 371–383.

11. Jin, G. T., *Polygon indices and the superbridge indices of torus knots and links,* Journal of Knot Theory and its Ramifications **6** no.2 (1997), 281–289.

12. Kuiper, N. H., *A new knot invariant,* Mathematische Annalen **278** (1987) 193–209.

13. Lickorish, W. B. R. and K. C. Millett, *A polynomial invariant of oriented links,* Topology **26** no.1 (1987) 107–141.

14. _____, *The new polynomial invariants of knots and links,* Mathematics Magazine **61** no.1 (1988) 3–23.

15. Meissen, M., *Edge number results for piecewise-linear knots, Knot Theory,* Banach Center Publications Vol.42, Polish Academy of Sciences, Institute of Mathematics, Warsaw (1998).

16. _____, *Lower and upper bounds on edge numbers and crossing numbers of knots,* Ph.D. thesis, University of Iowa (1997).

17. Millett, K. C. and D. W. Sumners (eds.), *Random Knotting and Linking,* Series on Knots and Everything Vol.7, World Scientific, Singapore (1994).

18. Millett, K. C., *Knotting of regular polygons in 3-space,* Journal of Knot Theory and its Ramifications **3** no.3 (1994) 263–278; also in *Random Knotting and Linking,* K. C. Millett and D. W. Sumners (eds.), Series on Knots and Everything Vol.7, World Scientific, Singapore (1994) 31–46.

19. Negami, S., *Ramsey theorems for knots, links, and spatial graphs,* Transactions of the American Mathematical Society **324** (1991) 527–541.

20. Przytycka, T. M., and J. H. Przytycki, *Subexponentially computable truncations of Jones-type polynomials, Graph Structure Theory,* Contemporary Mathematics Vol.147, American Mathematical Society, Providence, Rhode Island (1993) 63–108.

21. Randell, R., *A molecular conformation space,* MATH/CHEM/COMP 1987, R. C. Lacher (ed.), Studies in Physical and Theoretical Chemistry **54** (1988) 125–140.

22. _____, *Conformation spaces of molecular rings,* MATH/CHEM/ COMP 1987, R. C. Lacher (ed.), Studies in Physical and Theoretical Chemistry **54** (1988) 141–156.

23. _____, *An elementary invariant of knots,* Journal of Knot Theory and its Ramifications **3** no.3 (1994) 279–286; also in *Random Knotting and Linking,* K. C. Millett and D. W. Sumners (eds.), Series on Knots

and Everything Vol.7, World Scientific, Singapore (1994) 47–54.

24. Scharein, R. G., *Interactive topological drawing,* Ph.D. thesis, University of British Columbia (1998).

25. Sumners, D. W. (ed.), *New Scientific Applications of Geometry and Topology,* Proceedings of Symposia in Applied Mathematics Vol.45, American Mathematical Society, Providence, Rhode Island (1992).

26. Vassiliev, V. A., *Complements of Discriminants of Smooth Maps: Topology and Applications*, Translations of Mathematical Monographs Vol.98, American Mathematical Society, Providence, Rhode Island (1992).

27. Whitney, H., *Elementary structure of real algebraic varieties,* Annals of Mathematics (Second Series) **66** (1957) 545–556.